RSC Advances

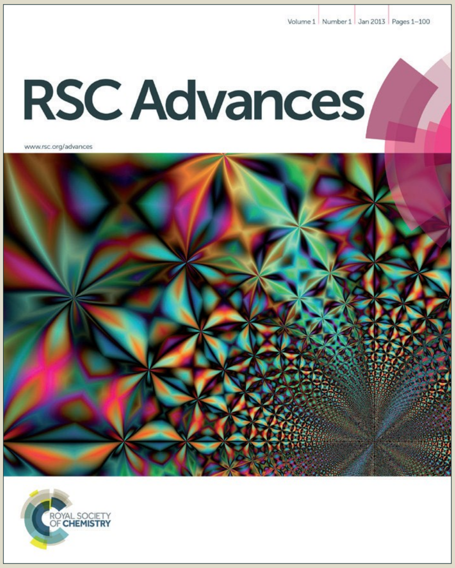

ROYAL SOCIETY OF CHEMISTRY

www.rsc.org/advances

RSC Advances RSCPublishing

ARTICLE

Cite this: DOI: 10.1039/x0xx00000x

Received 00th January 2012,
Accepted 00th January 2012

DOI: 10.1039/x0xx00000x

www.rsc.org/

Oxidative Dehydrogenation of 1-Butene over Vanadium Modified Bismuth Molybdate Catalyst: An Insight into Mechanism

Chao Wan [a, b], Dang-guo Cheng [b,*], Fengqiu Chen [a, b] and Xiaoli Zhan [b]

$BiMoV_x$ catalysts (x=0–0.3) were prepared by co-precipitation method and investigated in the oxidative dehydrogenation (ODH) of 1-butene to 1,3-butadiene. The results show that the vanadium content has significant effects on the catalyst performance and $BiMoV_{0.15}$ exhibits the superior activity. X-ray photoelectron spectroscopy (XPS) and Temperature programmed re-oxidation (TPRO) indicate that the oxygen mobility of catalysts is one of crucial factors determining catalytic performance in ODH reaction. The mechanism of oxygen migration in ODH reaction is discussed and proposed.

Introduction

Recently, the oxidative dehydrogenation (ODH) of light paraffin has attracted much attention due to growing demand for light olefins such as 1,3-butadiene (BD). It is an important raw material for manufacturing a large number of chemical products [1,2]. Several metal oxides have been investigated in ODH of n-butene to BD, including vanadium-containing catalyst [3], ferrite-type catalyst [4], manganese oxide molecular sieve [5], Cu-Mo catalyst [6] and bismuth molybdate [7,8]. Among these catalysts, bismuth molybdate exhibited the promising catalytic performance [7-11]. The present investigation reveals that ODH of n-butene to BD over bismuth molybdate follows the Mars–van Krevelen mechanism [12-15]. That is lattice oxygen in the catalyst reacts with n-butene and produces water and BD firstly. And then molecular oxygen in the gas phase makes up oxygen vacancy in the catalyst [16-18]. This implies that oxygen mobility is one of the vital factors determining the catalytic performance of bismuth molybdate in ODH of n-butene.

As a result, much effort has been taken to enhance the oxygen mobility of bismuth molybdate by adding some promoters, which can be categorized into two groups. One is to substitute Bi in the catalysts with other metal atoms partially. The other one is to replace Mo atom in bismuth molybdates. Currently, the metal for Bi atom in bismuth molybdate includes Co, Fe and Ni, and etc [10,14,19,20]. While P was employed for the substitution of Mo atom [10,21]. Based on these studies, it is found that the enhancement of oxygen mobility is due to the formation of some new crystal phases between the promoter and Bi or Mo. The intrinsic mechanism is that lattice oxygen in the formed phases is easy to react with n-butene to produce oxygen vacancy. The oxygen mobility is strongly related to these vacancies.

In this regard, we have prepared La-modified bismuth molybdate and investigated its performance in ODH of n-butene previously [22]. Our prepared catalysts showed good catalytic activity in the reaction due to the substitution of Bi with La. And La is well known for its capability to store and release oxygen and low-temperature reducibility [23]. Although extensive researches have been conducted aiming at the improvement of oxygen mobility of bismuth molybdate by the addition of the third metal [8,14,19-22]. But some important issues are still not clear. For example, the bulk structure modification of catalyst related to the promoter addition will influence the formation of oxygen vacancy inevitably. Some oxygen migration during ODH reaction will happen in the bulk due to the different bonding energy between metal and oxygen. Further insight into the mechanism of oxygen mobility can provide useful information for screening more effective promoter, which is still an interesting research topic in ODH reaction.

In this work, we employed vanadium as promoter to replace the Mo in bismuth molybdate and a series of $BiMoV_x$ with different vanadium contents (x=0-0.3) were prepared by co-precipitation method. Vanadium is the metal with mixed-valence state which shows good activity in some dehydrogenation reaction [21,24-26]. The prepared catalysts were investigated in ODH of 1-butene to BD. $BiMoV_x$ catalysts were characterized by using X-ray diffraction (XRD), X-ray photoelectron spectroscopy (XPS) and Temperature-programmed re-oxidation (TPRO). The relationship between the catalytic activity and vanadium content in the catalysts was discussed, the oxygen mobility as well. The route of oxygen migration in the catalysts for ODH reaction was proposed.

---

[a] *Key Laboratory of Biomass Chemical Engineering of Ministry of Education, Zhejiang University, 38 Zheda Road, Hangzhou 310027, China*

[b] *College of Chemical and Biological Engineering, Zhejiang University, 38 Zheda Road, Hangzhou 310027, China*

E-mail address: dgcheng@zju.edu.cn (D.G. Cheng)

Tel.: +86 571 87953382; Fax: +86 571 87951227

Experimental

Preparation of BiMoV$_x$ catalysts

BiMoV$_x$ catalysts (x=0-0.3) were prepared by conventional co-precipitation method. The desired amount of ammonium meta-vanadate solution (NH_4VO_3) was dissolved in deionized water at 70 °C and added dropwise into ammonium molybdate solution ($(NH_4)_6Mo_7O_{24}\cdot 4H_2O$) under vigorously stirring. Afterwards, bismuth nitrate solution ($Bi(NO_3)_3\cdot 5H_2O$) acidified with 10% nitric acid was added dropwise into the above-mentioned mixture. The mixture was adjusted to pH 5 by aqueous 27 wt% NH_4OH and aged at room temperature for 4 h and then stirred to viscous solid at the water bath to remove the excess water. The resulting viscous solid was dried at 80 °C overnight and calcined at 550 °C for 2 h in an air atmosphere. The catalysts are designated as BiMoV$_x$ catalysts (x= 0–0.3), where x is the molar ratio of vanadium in the catalyst.

Catalyst Characterization

X-ray powder diffraction (XRD) patterns of BiMoV$_x$ were recorded on XRD 6000 equipped with Cu Kα radiation at 40kV and 30mA. Data were collected in the 2θ range of 10-50° with a scan rate of 1°min^{-1}. Elemental composition of the prepared catalysts was determined by ICP-AES (Thermo iCAP6300) analyses. The BET surface area and pore volume of the catalysts were measured using N2 as a sorbate at 77 K in a static volumetric apparatus (Micromeritics ASAP2020). The relationship between oxygen mobility and vanadium content was also investigated through the temperature-programmed re-oxidation (TPRO) on fixed-bed apparatus attached to a Hiden QIC-20 quadruple mass spectrometer. For the temperature programmed reduction by 1-butene, 0.2 g catalyst was pretreated at 440 °C for 1 h in flowing 1-butene (20 cm^3·min^{-1}), held for 2h at that temperature and then cooled to room temperature in flowing He (30 cm^3·min^{-1}). Subsequent temperature programmed oxidation was performed in flowing 2% O_2/He (30 cm^3·min^{-1}) from room temperature to 600 °C at 10 °C·min^{-1}. X-ray photoelectron spectroscopy (XPS) spectra for BiMoV$_x$ catalysts were conducted by using an Escalab 250Xi XPS system. An Mg *Kα* anode was used as the X-ray source. The binding energy of the electron, correcting charge effects, was calibrated with respect to the signal of the adventitious carbon (binding energy: 284.6 eV). Spectrum deconvolution was carried out using the spectra of X-ray satellite peak subtraction and background correction.

Catalytic measurement

Catalytic tests were performed in a tubular fixed-bed reactor (i.d. = 8 mm) with 1.5 g catalyst under atmospheric pressure. The prepared catalysts were pressed into 40-60 mesh for testing. Prior to the reaction, the catalyst was routinely activated with flowing air stream (50 cm^3·min^{-1}) at 440 °C for 2 h. The water feed was continuously vaporized by passing through a pre-heating zone at 120°C and fed into the reactor together with 1-butene and air. The feed composition was fixed at a ratio of 1-butene: oxygen: steam=1:0.8:10 with total gas flow rate of 112.5 cm^3·min^{-1}. The reactants and products were analyzed by on-line gas chromatography with two columns. Hydrocarbons were analyzed using a KB-Al_2O_3/Na_2SO_4 column with a FID detector, and CO and CO_2 by a TDX-01 column with a TCD detector.

Results and discussion

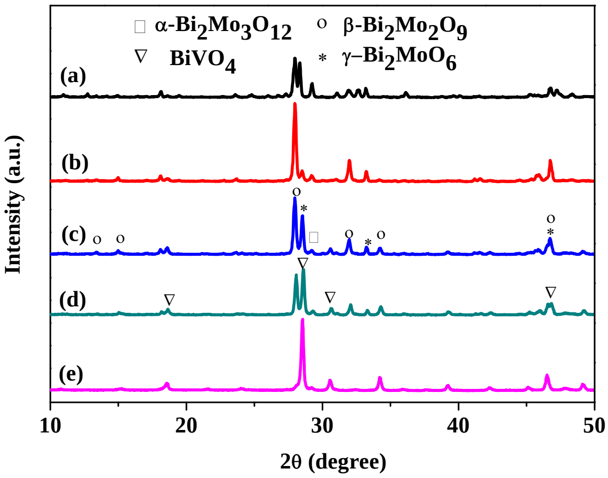

Fig. 1 XRD patterns of BiMoV$_x$ catalysts with different V content; (a) x in BiMoV$_x$ catalysts = 0, (b) 0.1, (c) 0.15, (d) 0.2, and (e) 0.3

Table 1 Structural property of BiMoV$_x$ catalysts.

Catalyst	Atomic ratio [a]			S_{BET} (m^{2}g^{-1})	Pore volume(cm^{3}g^{-1})	Oxygen consumption of first peak in TPRO (μmol/g)	Total oxygen consumption in TPRO(μmol/g)
	Bi	Mo	V				
BiMo	1	0.98	0	1.2	0.011	15.4	40.6
BiMoV$_{0.1}$	1	0.97	0.09	1.4	0.014	13.2	44.8
BiMoV$_{0.15}$	1	0.96	0.14	2.3	0.018	11.7	51.2
BiMoV$_{0.2}$	1	0.99	0.21	1.5	0.019	12.5	46.5
BiMoV$_{0.3}$	1	1.00	0.28	1.1	0.007	8.5	43.2

[a] Determined by ICP-AES

RSC Advances RSCPublishing

ARTICLE

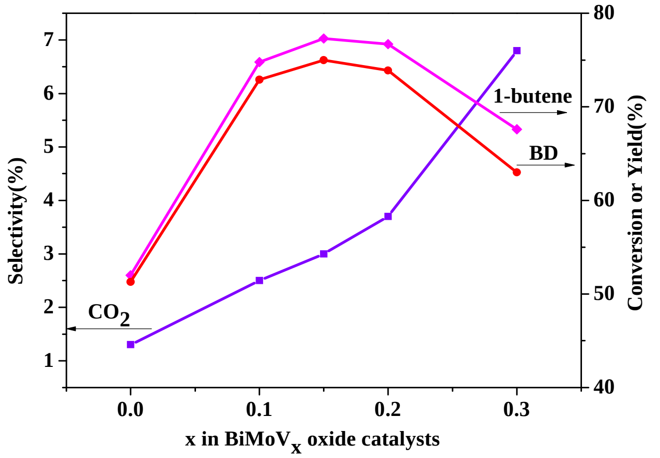

Fig. 2 Catalytic performance of BiMoV$_x$ catalysts as a function of V content in ODH of 1-butene

XRD patterns of BiMoV$_x$ catalysts with different vanadium content are shown in Fig. 1. Three solid phases of α-$Bi_2Mo_3O_{12}$, β-$Bi_2Mo_2O_9$, and γ-Bi_2MoO_6, coexisting with a minor amount of the $BiVO_4$ phase, can be detected in the prepared samples. Trifiro *et al.* demonstrate that Mo=O is related with the selectivity activity center of catalyst while Mo−O−Mo acts as total oxidation center in bismuth molybdate oxides [27-29]. In BiMoV$_x$ catalysts, the structure and circumstance of Mo=O are modified by the incorporation of the component vanadium. V is in the tetrahedral VO_4 structure [28-32]. This probably implies that Mo in the lattice position is replaced partially by V in BiMoV$_x$ oxide catalysts.

BET surface area, total pore volume and elemental composition of the BiMoV$_x$ oxide catalysts are shown in Table 1. The surface areas of the catalysts are found to be very low (1.1–2.3 m^2/g), as reported in the previous works [21]. And there is no consistent trend with a variation of vanadium content. Elemental analysis by ICP-AES indicates that the actual content of each metal are in good agreement with that of the expected one experimentally. This result also confirms the successful preparation of BiMoV$_x$ oxide in this work.

The prepared catalysts were investigated in ODH of 1-butene at 440 °C for 2 h. Three types of compounds are detected including dehydrogenation products (BD), isomerization products (trans and cis-2-butene) and combustion products (CO and CO_2). The cracking products (CH_4, C_2H_4, C_2H_6, C_3H_6 and C_3H_8) are almost negligible. BD and CO_2 are dominating products. Fig. 2 plots the tendency of BiMoV$_x$ oxides activity *vs.* vanadium content. One can see that the selectivity for CO_2 is increased with the increase of the vanadium content. However, it is noticeable that conversion of 1-butene and yield for BD show volcano curves with respect to vanadium content. BiMoV$_{0.15}$ shows the optimal catalytic performance in this work.

It has been reported that the oxygen mobility of bismuth molybdenum catalyst is one of crucial factors to catalytic performance in ODH reaction. In order to clarify the relationship between the catalytic performance and the oxygen mobility of BiMoV$_x$, XPS and TPRO analysis are conducted. XPS analyses are carried out to determine oxygen mobility of the catalyst by measuring the binding energies of O 1s of BiMoV$_x$ catalyst. Fig. 3(A) depicts deconvolution of the O 1s spectrum of BiMoV$_{0.15}$ catalyst. Deconvolution of O 1s spectrum reveals that there are three types of surface oxygen species in the BiMoV$_{0.15}$ catalyst (denoted as Type-I, -II, and -III in the order of increasing binding energy). As literature reported [9-13,33], Type-I oxygen with the lowest binding energy (530.3 eV) is attributed to be the oxygen species strongly bonded to the metal component in the catalyst, type-III oxygen with the highest binding energy

Table 2 Binding energies of O 1s of BiMoV$_x$ oxide catalysts

Catalyst	Binding energy (eV) of O 1s		
	Type-I	Type-II	Type-III
BiMo	530.3	531.1	533.1
BiMoV$_{0.1}$	530.2	531.6	532.8
BiMoV$_{0.15}$	530.3	531.8	532.5
BiMoV$_{0.2}$	530.3	531.7	533.1
BiMoV$_{0.3}$	530.3	531.4	532.6

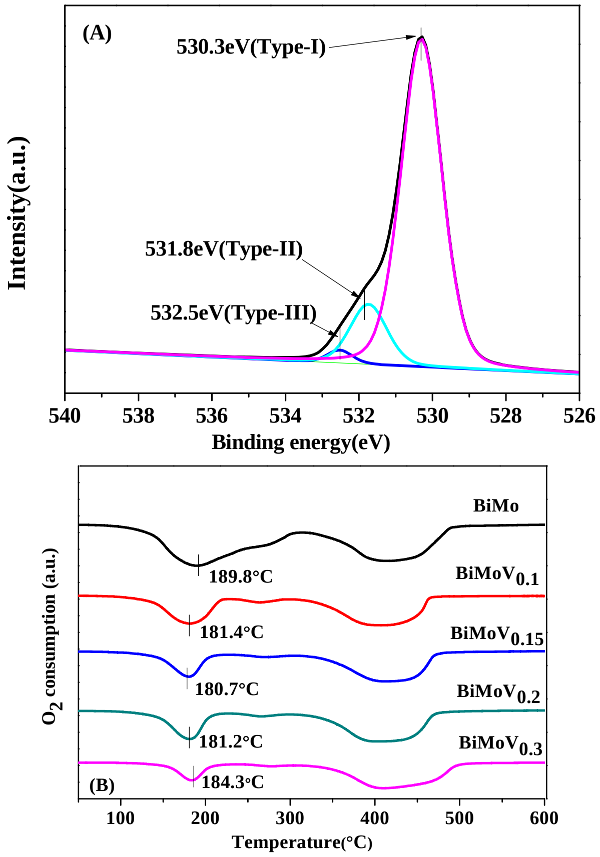

Fig. 3 (A) Deconvolution of the O 1s spectrum of BiMoV$_{0.15}$ oxide catalysts and (B) TPRO profiles of partially reduced BiMoV$_x$ catalysts

(532.5–533.1 eV) corresponds to the oxygen species weakly bonded on the catalyst surface. Type-II oxygen reflects the oxygen mobility of the multicomponent bismuth molybdate catalyst [33]. Table 2 summarizes the binding energy of deconvolution of O 1s spectrum of $BiMoV_x$ catalysts. It is generally believed that only the binding energy of type-II oxygen is used as an index for the oxygen mobility of the multicomponent bismuth molybdates catalyst [33]. The higher binding energy of Type-II oxygen is, the higher the oxygen mobility is.

TPRO analysis is also conducted to estimate oxygen mobility of the catalyst by testing the peak temperature in TPRO. Prior to TPRO analysis, catalysts were pretreated with flowing 1-butene at 440 °C for 3 h. Fig. 3 (B) shows the TPRO profiles of $BiMoV_x$ catalysts. The profiles for each catalyst consist of two oxidation peaks. It is widely believed that the peak temperature in TPRO indicates the capacity of oxygen mobility on bismuth molybdenum oxides. The lower the temperature is, the easier the oxygen mobility is. The total oxygen consumption in TPRO is related with catalytic performance and reflects the capability for oxygen make-up. The total oxygen quantity can be calculated by TPRO total peak area, as displayed in Table 1. The more the total oxygen consumption is, the easier the oxygen mobility is. $BiMoV_{0.15}$ with the total oxygen quantity of 51.2 μmol/g exhibits optimal catalytic activity. These results are well consistent with the trend of binding energy of Type-II oxygen in Table 2.

Fig. 4 demonstrates a comprehensive correlation between the yield for BD and the oxygen mobility of $BiMoV_x$ catalysts. It is evident that the yield increases linearly with the increase of oxygen mobility. This result implies that the catalytic activity could be improved with increasing oxygen mobility of the catalyst. Therefore, the catalysts of $BiMoV_{0.15}$ displays the superior activity as result of its higher binding energy of Type-II oxygen and lower TPRO temperature compared to the others prepared catalysts [17-19, 33].

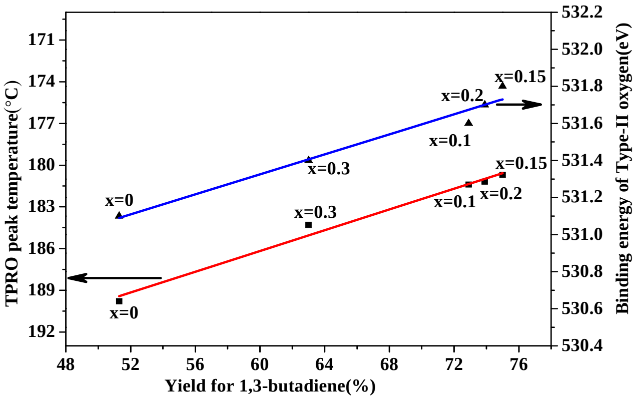

Fig. 4 A comprehensive correlation between catalytic performance and oxygen mobility of $BiMoV_x$ in the ODH of 1-butene to 1,3-butadiene: x in $BiMoV_x$ oxide catalysts= 0, 0.1, 0.15, 0.2, and 0.3

To assign the oxygen consumption in TPRO profiles, the effluent gas during testing $BiMoV_{0.15}$ is analyzed by a Hiden QIC-20 quadruple mass spectrometer. The gas composition is mainly composed of O_2 and CO_2, as displayed in Fig. 5. In the low temperature at *ca.* 180.7 °C, there is no CO_2 formed indicating the composition of oxygen may be related to the oxidation of metal species partially reduced by n-butene. The second small peak is the combustion of coke on the catalyst surface, as some literatures reported [19,21,33]. And the O_2 consumption at the high temperature at *ca.* 410.7 °C may be correlated with the oxidation of metal species and the combustion of coke on the catalyst surface.

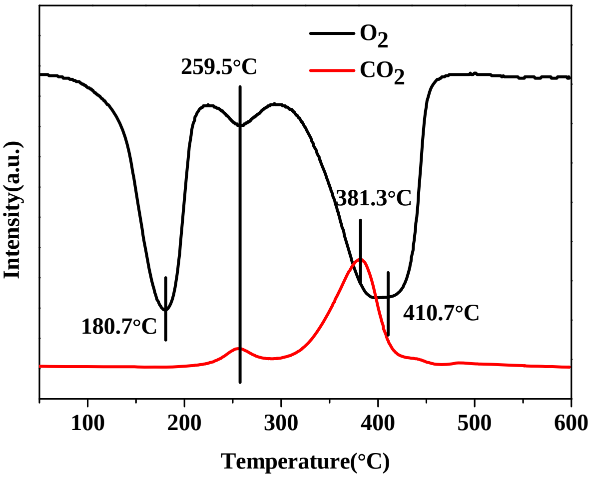

Fig. 5 MS signals of TPRO of $BiMoV_{0.15}$ oxide catalyst; m/z =32 (•O_2), 44(•CO_2) were recorded during TPRO analysis

Table 3. Three typical samples used for XPS characterization

Sample	Description
$BiMoV_{0.15}$-440	$BiMoV_{0.15}$ pretreated by 1-butene at 440 °C for 2 h
$BiMoV_{0.15}$-200	$BiMoV_{0.15}$ oxidized in TPRO when the temperature reaches to 200 °C
$BiMoV_{0.15}$-600	$BiMoV_{0.15}$ oxidized in TPRO when the temperature reaches to 600 °C

From above analysis, the vanadium addition can improve ODH performance of bismuth molybdate significantly due to the enhancement of oxygen mobility. The assignment of oxygen consumption in TPRO tests indicate that the evolution of oxyge vacancy during the reaction, which may result from the oxygen migration. To elucidate the intrinsic mechanism, three typical samples, described in Table 3, at different stage of TPRO test were collected and characterized by XPS. As shown in Fig. 6, the shape of the Mo3$d_{5/2}$ spectrum remains unchanged from $BiMoV_{0.15}$-440 to $BiMoV_{0.15}$-200, however, the shape of the Mo3$d_{5/2}$ spectrum make a distinct change from $BiMoV_{0.15}$-200 to $BiMoV_{0.15}$-600. Deconvolution of the Mo3*d* spectrum in Fig. 6a produce three kinds of core spectra of Mo3$d_{5/2}$= 232.5, 231.3, and 229.4eV. The first core spectrum of 232.5 eV is related to Mo^{6+} [34-36]. The second one is ascribed to Mo^{5+}. The last one is accord with Mo^{4+} reported by Cimino and Angelis [37]. Grzybowska *et al.* have also reported the appearance of Mo^{4+} on bismuth molybdates treated in 470°C at reducing atmosphere [38]. Nevertheless, deconvolution of the Mo3*d* spectrum in Fig. 6c produce only core spectra of Mo3$d_{5/2}$= 232.5eV, this means the catalysts is merely composed of Mo^{6+}. Therefore, [illegible] can be inferred that the high temperature peak one in the range of 400–500 °C is ascribed to the oxidation process of molybdenum [19,39,40]. Fig. 7 shows V2*p* spectra obtained in different samples. The shape of the V2$p_{3/2}$ spectrum remains unchanged from $BiMoV_{0.15}$ 440 to $BiMoV_{0.15}$-200, two kinds of V2$p_{3/2}$ can be observed, the fir spectrum of 516.9 eV is related to V^{5+}. The second spectrum of 515.9 eV corresponds to V^{4+}.The similar phenomenon is reported in literature [41,42]. It is evident that the second spectrum of 515.9eV disappears in BiMoV$_{0.15}$-600, it can be deduced that the valence state of V^{4+} is oxidized to V^{5+}.Therefore, the high temperature peak may be attributed to the oxidation process of vanadium. Therefore, the oxygen consumption at high temperature peak in TPRO may be correlated with the oxidation process of both molybdenum and vanadium.

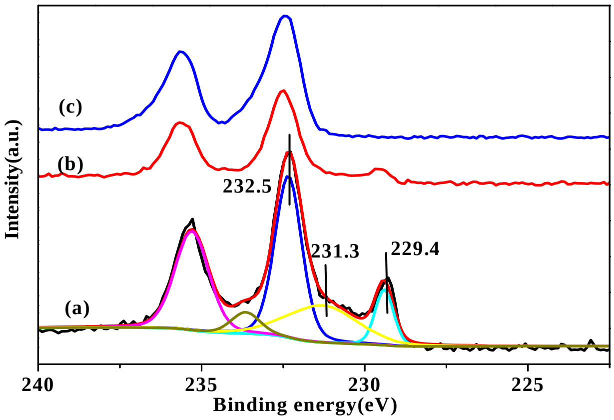

Fig. 6 Mo 3*d* signals of different sample (a) BiMoV$_{0.15}$-440; (b) BiMoV$_{0.15}$-200; (c) BiMoV$_{0.15}$-600

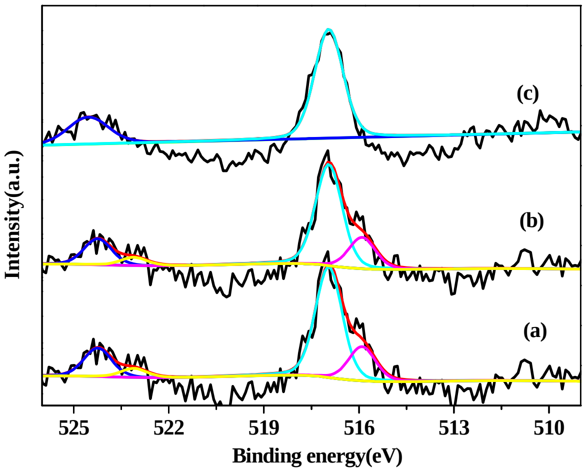

Fig. 7 V 2*p* signals of different sample (a) BiMoV$_{0.15}$-440; (b) BiMoV$_{0.15}$-200; (c) BiMoV$_{0.15}$-600

XRD characterization was used to analyze the bulk structure changes during TPRO test, as shown in Fig. 8. One can see that the patterns of the BiMoV$_{0.15}$ oxide catalysis change significantly from BiMoV$_{0.15}$-440 to BiMoV$_{0.15}$-200. For BiMoV$_{0.15}$-440, there is a clear diffraction peak of metal Bi, the characteristic diffraction angle of Bi is 27.2 °, 37.9 °, 39.6 °. However, for BiMoV$_{0.15}$-200, no diffraction peaks of Bi are observed. These results suggest that the lattice oxygen bonded to Bi reacts with 1-butene during the pretreatment totally. Grzybowska *et al.* [38] have also reported that metallic bismuth or Bi^0 is formed along with the reduced molybdenum cations in vigorous or excessive reduction. Thus, it is reasonable to deduce that the low temperature peak of TPRO profiles in the range of 150–200 °C ascribe to the oxidation of bismuth species. But for Mo and V species, no characteristic peaks can be observed. The reason may be due to the low diffraction of their oxides.

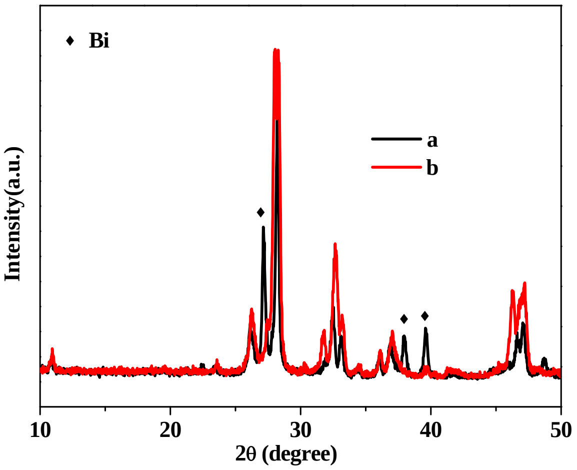

Fig. 8 XRD patterns of different sample (a) BiMoV$_{0.15}$-440; (b) BiMoV$_{0.15}$-200

Based on our experimental results and references reported [9,14,39,40], we can deduce the metal valence changes during the reaction, as Table 4 summarized. For fresh BiMoV$_{0.15}$, four solid phases including α-Bi$_2$Mo$_3$O$_{12}$, β-Bi$_2$Mo$_2$O$_9$, γ-Bi$_2$MoO$_6$, and BiVO$_4$ can be found (Fig.1), which indicates the valence of Bi, Mo, and V is +3, +6, and +5, respectively. After reduced by 1-butene, the significant changes occur. Bi^{+3} turns into metallic Bi because the oxygen coordinated is captured by 1-butene completely (Fig.8). But in the case of Mo and V, the valence of former one changes to +5, +4 and the latter to +4 (Fig.6 and 7). These suggest that not all of oxygen around Mo and V participate in the reaction. The energy of the metal component bonded to the oxygen is responsible for these differences, which will lead to the oxygen migration during the ODH reaction.

Table 4. Metal valence changes on BiMoV$_{0.15}$ during reaction.

Sample	Bi	Mo	V
BiMoV$_{0.15}$	+3	+6	+5
BiMoV$_{0.15}$-440	0	+5,+4	+5,+4
BiMoV$_{0.15}$-200	+3	+5,+4	+5,+4
BiMoV$_{0.15}$-600	+3	+6	+5

It is well known that the oxidative dehydrogenation of 1-butene over bismuth molybdate catalyst follows the Mars-van Krevelen mechanism[19-22]. According to this mechanism, oxygen in the catalyst directly reacts with 1-butene, and in turn, oxygen in the gas phase makes up oxygen vacancy in the catalyst. The transformation of oxygen between the gas phase and catalyst surface will lead to the valence changes of metal surrounding oxygen inevitably. The changes of metal valence on the catalysts during the different stage of reaction can give us an indirect understanding of oxygen migration in the reaction, as Fig. 9 proposed. 1-Butene reacts with surface oxygen atom bonding to metal on the catalysts firstly. But the oxygen around Bi may be captured preferentially due to the low energy between them. With the reaction taking place, oxygen vacancy is formed. Then there is the oxygen migration between Bi and Mo, V for the difference from the bonding energy. But if 1-butene is only react with oxygen atom in the surface and near-surface regions of catalysts, the peak of consumption of oxygen in TPRO will be not so obvious. Therefore, there must be the occurrence of oxygen migration in the catalysts. It can be evolved that the bulk lattice oxygen transfers into the surface to participate in ODH reaction following the direction of arrows. The Bi metal species in the bulk regions is also reduced. There are many oxygen vacancy formed in the catalysts with the oxidative dehydrogenation proceed. Afterward, oxygen vacancy in the surface and near-surface of catalysts will be filled by gas oxygen. In view of the difference of peak temperature in TPRO, the Bi metal species in the surface and near-surface of catalysts is oxidized firstly. As the reaction continues, the oxygen species around Bi enrich. Then the Mo and V metal species in the bulk regions is also oxidized. Consequently, the whole process is circulated repeatedly of ODH process and oxygen migration process. Our results demonstrate the introduction of V in BiMo catalysts strengthen the oxygen migration process and oxygen mobility subsequently.

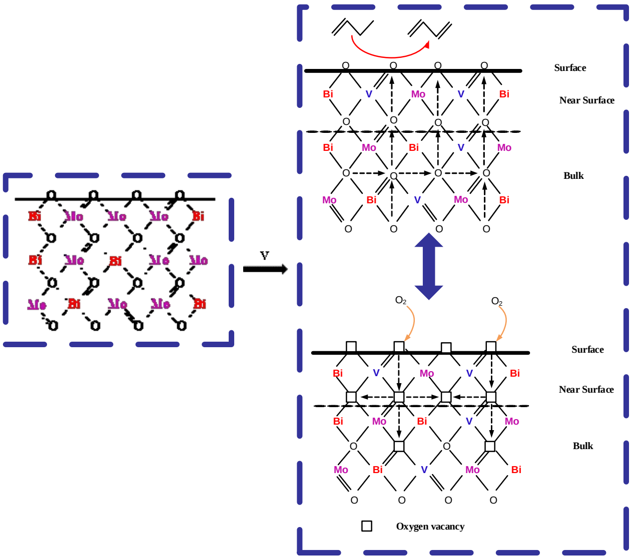

Fig. 9 Reaction mechanism and oxygen migration process of this reaction

Conclusions

In this work, $BiMoV_x$ with different vanadium content have been tested in ODH of 1-butene to BD. Conversion of 1-butene and yield for BD over $BiMoV_x$ catalysts show volcano-shaped curves with respect to vanadium content. The characterization results reveal that the catalytic performance could be enhanced by increasing oxygen mobility of the catalyst. This factor leads the better activity of $BiMoV_{0.15}$ than that of the others. The reason of temperature peak in TPRO profile is investigated, and the first peak of TPRO profiles could be assigned to the oxidation of bismuth species and the second peak is attributed to the oxidation process of molybdenum and vanadium. The oxygen migration between Bi and Mo, V take place during the reaction due to the difference from the bonding energy between metal and oxygen, the migration from bulk to surface as well. This work demonstrates that the introduction of element with high oxygen mobility can improve the performance of catalyst for ODH reaction effectively. It provides useful information for future catalysts designs. Moreover, $BiMoV_x$ catalyst is expected to be applied in oxidative dehydrogenation of other hydrocarbons.

Acknowledgements

Financial supports from Zhejiang Provincial Natural Science Foundation (LZ13B060004) and the Program for Zhejiang Leading Team of S&T Innovation (2013TD07) are gratefully appreciated.

Notes and references

1 F. Hong, B. L. Yang, L. H. Schwartz and H. H. Kung, *J. Phys. Chem.*,1984, **88**, 2525-2530.
2 W. J. Yan, Q. Y. Kouk, J. Z. Luo, Y. Liu and A. Borgna, *Catal. Commun.*,2014, **46**, 208–212.
3 J. M. López Nieto, P. Concepción, A. Dejoz, H. Knözinger, F. Melo a M. I. Vázquez, *J. Catal.*, 2000, **189**, 147-157.
4 H. Lee, J. C. Jung, H. Kim, Y. M. Chung, T. J. Kim, S. J. Lee, S. H. Oh, Y. S. Kim and I. K. Song, *Catal. Commun.*, 2008, **9**, 1137-1142.
5 V. V. Krishnan and S. L. Suib, *J. Catal.*, 1999, **184**, 305-315.
6 P. N. Tiwari, T. G. Alkhazov, K. U. Adzamov and A. K. Khanmamedova, *J. Catal.*, 1989, **120**, 278-281.
7 D. A. G. van Oeffelen, J. H. C. van Hooff and G. C. A. Schuit, *J. Catal.*, 1985, **95**, 84-100.
8 J. C. Jung, H. Kim, Y. S. Kim, Y. M. Chung, T. J. Kim, S. J. Lee, S. H. Oh and I. K. Song, *Appl. Catal. A-Gen.*, 2007, **317**, 244-249.
9 Y. Moro-oka and W. Ueda, *Adv. Catal.*, 1994, **40**, 233-273.
10 D. G. Filkova, L. A. Petrov and D. M. Shopov, *J. Catal.*, 1984, **88**, 119-124.
11 A. P. V. Soares, L. D. Dimitrov, M. C. A. Oliveira, L. Hilaire, M. F. Portela and R. K. Grasselli, *Appl. Catal. A-Gen.*, 2003, **253**, 191-200.
12 M. F. Porteal, *Top. Catal.*, 2001, **15**, 241-245.
13 R. K. Grasselli, in: G. Ertl, H. Knözinger, J. Weitkamp (Eds.), *Handbook of Heterogeneous Catalysis*, vol. 5, Wiley, New York, 1997, pp. 2302-2326.
14 J. C. Jung, H. Lee, H. Kim, S. Park, Y. M. Chung, T. J. Kim, S. J Lee, S. H. Oh, Y. S. Kim and I. K. Song, *Catal. Commun.*, 2008, **9**, 2059-2062.
15 Ph. A. Batist, A. H. W. M. Der Kinderen, Y. Leeuwenburgh, F. A. M. G Metz and G. C. A. Schuit, *J. Catal.*, 1968, **12**, 45-60.
16 E. Ruckenstein, R. Krishnan and K. N. Rai, *J. Catal.*, 1976, **45**, 270-273.
17 G. C. A. Schuit, *J. Less Commun. Met.*, 1974, **36**, 329-338.
18 W. Ueda, Y. Moro-oka and T. Ikaws, *J. Catal.*, 1984, **88**, 214-221.
19 J. H. Park, K. Row and C. H. Shin, *Catal. Commun.*, 2013, **31**, 76-80.
20 M. W. J. Wolfs and Ph. A. Batist, *J. Catal.*, 1974, **32**, 25-36.
21 J. H. Park and C. H. Shin, *Appl. Catal. A: Gen.*,2015, **495**, 1–7.
22 C. Wan, D. G. Cheng, F. Q. Chen and X. L. Zhan, *Chem. Eng. Sci.*, 20 in press. doi:10.1016/j.ces.2014.08.020.
23 Y. W. Zhang, Y. M. Zhou, M. H. Tang, X Liu and Y. Z. Duan, *Chem. Eng. J*, 2012, **181–182**, 530–537.
24 K. Fukudome, N. Ikenaga, T. Miyake and T. Suzuki, *Catal. Sci. Technol.*, 2011, **1** , 987–998.
25 N. R. Shiju, M. Anilkumar, S. P. Gokhale, B. S. Rao and C. V. V. Satyanarayana, *Catal. Sci. Technol.*, 2011, **1** , 1262–1270.

26 S. Sokolov, M. Stoyanova, U. Rodemerck, D. Linke and E. V. Kondratenko. *Catal. Sci. Technol.*, 2014, **4**, 1323-1332.

27 F. Trifiro, I. Pasquon, *J. Catal.*, 1968, **12**, 412− 416.

28 A. Nell, A. Getsoian, S. Werner, L. Kiwi-Minsker and A. T. Bell. *Langmuir*, 2014, **30**, 873–880.

29 Z. Zhai, A. Getsoian and A.T. Bell, *J. Catal.*, 2013, **308**, 25–36.

30 C. G. Barraclough, J. Lewis and R. S. Nyholm, *J. Chem. Soc.*, 1959, 3552− 3555.

31 F. D. Hardcastle and I. E. Wachs, *J. Phys. Chem.*, 1991, **95**, 5031− 5041.

32 H. P. Yang, Y. N. Fan, L. Y. Feng, J. H. Qiu, M. Lin, B. L. Xu and Y. Chen, *Acta Chim. Sinica*, 2002, **60**, 1006− 1010.

33 J. C. Jung, H. Lee, H. Kim, Y. M. Chung, T. J. Kim, S. J. Lee, S. H. Oh, Y. S. Kim and I. K. Song, *Catal. Commun.*, 2008, **9**, 943-949.

34 K. Uchida and A. Ayame, *J. Surf. Sci. Soc. (in Japanese)*, 1994, 15, 393−399.

35 K. Uchida and A. Ayame, *Surf. Sci.*, 1996, **170**, 357−358.

36 A. Ayame, M. Iwataya, K. Uchida, N. Igarashi and M. Miyamoto, *Jpn. J. Appl. Phys.*, 2000, **39**, 4335−4339.

37 A. Cimino and B. A. De Angelis, *J. Catal.*, 1975, **36**, 11−22.

38 B. Grzybowska, J. Haber, W. Marczewski and L. Ungier, *J. Catal.*, 1976, **42**, 327−333.

39 H. Miura, Y. Morikawa and T. Shirasaki, *J. Catal.*, 1975, **39**, 22–28.

40 J. H. Park, H. Noh, J. W. Park, K. Row, K. D. Jung and C. H. Shin, *Appl. Catal. A-Gen.*, 2012, **431-432**, 137-143.

41 S. Sugiyama, T. Hashimoto, Y. Tanabe, N. Shigemoto and H. Hayashi, *J. Mol. Catal. A: Chem.*, 2005, **227**, 255-261.

42 D. Gazzoli, S. De Rossi, G. Ferraris, G. Mattei, R. Spinicci and M. Valigi, *J. Mol. Catal. A: Chem.*, 2009, **310**, 17-23.

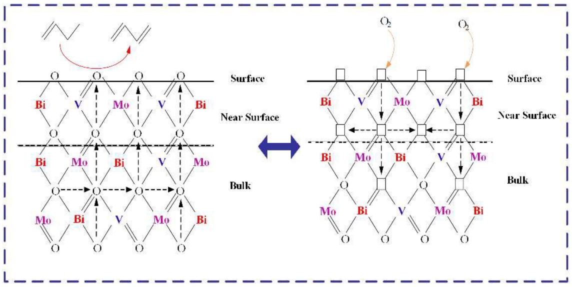

The effect of vanadium addition on the performance of bismuth molybdate catalysts has been discussed. The mechanism of oxygen mobility on the prepared catalysts is proposed.